IEEE Photonics Journal
An IEEE Photonics Society Publication

Surface-Plasma-Coupled Photovoltaic Cell With Double-Layered Triangular Grating

Volume 4, Number 3, June 2012

Yaohui Zhan
Jiupeng Zhao
Changhai Zhou
Xianjie Wang
Yanpeng Li
Yao Li

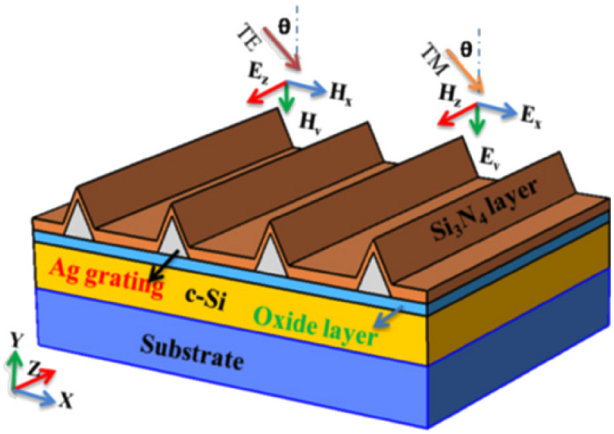

DOI: 10.1109/JPHOT.2012.2202221
1943-0655/$31.00 ©2012 IEEE

Surface-Plasma-Coupled Photovoltaic Cell With Double-Layered Triangular Grating

Yaohui Zhan,[1] Jiupeng Zhao,[2] Changhai Zhou,[1] Xianjie Wang,[3] Yanpeng Li,[1] and Yao Li[1]

[1]Center for Composite Materials, Harbin Institute of Technology, Harbin 150001, China
[2]School of Chemical Engineering and Technology, Harbin Institute of Technology, Harbin 150001, China
[3]Center for Condensed Matter Science and Technology, Harbin Institute of Technology, Harbin 150001, China

DOI: 10.1109/JPHOT.2012.2202221
1943-0655/$31.00 ©2012 IEEE

Manuscript received April 10, 2012; revised May 21, 2012; accepted May 24, 2012. Date of publication June 1, 2012; date of current version June 19, 2012. This work was partially supported by the State Key Program National Natural Science Foundation of China (No. 51010005, 90916020), and the Fundamental Research Funds for the Central Universities (HIT.ICRST.2010001). Corresponding authors: Y. Zhan and Y. Li (e-mail: yhzhan08@gmail.com; yaoli@hit.edu.cn).

Abstract: We present a plasmonic nanostructure design, integrated both of the metallic triangular grating and dielectric antireflection coatings, for ultrathin crystalline silicon solar cells. Considering both polarizations, the current improvement of the optimized structure can reach 76.8% under air mass 1.5 global illuminations. The mode analysis confirms that the enhanced optical absorption is attributed to improved coupling to both guided modes and localized modes. The absorption enhancement of such architecture is a little sensitive to the angle of incidence. The enhancement is still as high as 50% at 60 degrees of incidence.

Index Terms: Photovoltaic cell, surface plasma, triangular grating, surface plasmon polaritons (SPPs), localized surface plasmons (LSPs).

1. Introduction

Plasmonic photovoltaic is a very promising technology for improving solar cell efficiency and reducing its thickness [1]. The plasmonic structure utilizes localized and guided mode into photoactive layer of the solar cell. To excite the localized surface plasmons (LSPs) and surface plasmon polaritons (SPPs), many different plasmonic structures have been designed. Nobel spherical metal particles, e.g., silver [2], [3], gold [4], are widely used nowadays, which can be either laid on the top of solar cells [5] or embedded into the photoactive material [6]. Not only the feature size but also the shapes of particles are key factors in determining the coupling efficiency [7]. Then, besides the spherical shapes, a few of other geometries are proposed, e.g., nanodisk array [8], Au cylinder array [9], ellipsoid core-shell structure [10], rectangular grating [11], [12] and so on. The surface grating [13], volumetric grating [14], and back grating [15] have been applied into specific solar cells to improve the light absorption by 43%, 67% and 30%, respectively.

Previously, the use of double-layered plasmonic structures had been employed for tuning the surface plasmon dispersion frequency [16], [17], resulting the ability to engineer the peak of the Purcell enhancement factor. The use of triangular periodic grating leads to the ability to achieve improved light scattering at the interface of the device and air, which is similar to the increased light scattering in periodic structures used in light-emitting diodes [18], [19] and solar cells [20]. In addition, recent works have also reported the possibility of tuning the surface plasmon frequency by using 2-D

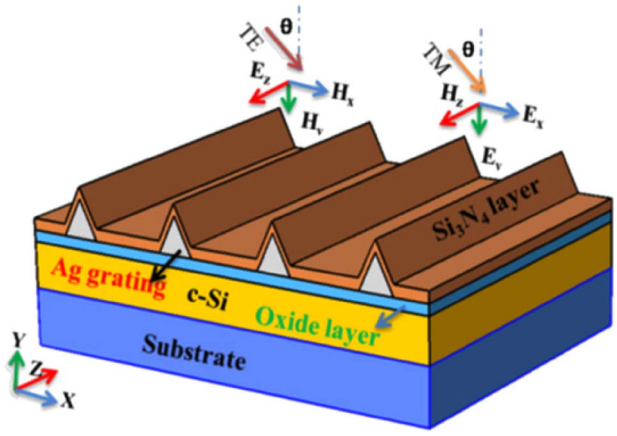

Fig. 1. Sketch of the DLTG solar cell.

lattice grating [21]. Furthermore, Munday and Atwater [22] considered rectangular gratings covered by an antireflection coating and demonstrated the importance of coupling to guided modes compared to localized modes.

However, most of the works about grating mentioned above have been directed at rectangular grating and the triangular grating is rarely reported. Moreover, leaving the metallic grating uncoated will increase the surface reflection, and consequently reduce the absorption of active layer. In this paper, we combine both metallic grating and antireflection coating together and propose a type of double-layered triangular grating (DLTG) array covering on plasmonic solar cells. Using full wave finite element method (FEM) modeling, we analyze how the polarization and angle of incident illumination affect the integrated absorption across the solar spectrum. We found that the optimized gratings greatly improve the light absorption in the photoactive region for a wide spectrum from 400 nm to 1100 nm. The absorption enhancement is verified to originate from mode coupling of both LSPs and SPPs.

2. Simulation Method

A sketch of the geometry is shown as Fig. 1. The periodic array of Ag triangular grating is coated with a layer of Si_3N_4 coating, which together are named DLTG for convenience. The unit cell of silver grating array is isosceles. The thickness of conformal Si_3N_4 layer is 45 nm, as [13]. The designed grating is covered on a silica-coated thin Si film (50 nm), supported by a silica substrate. The oxide layer is 10 nm and the substrate is infinite implemented by perfect match layer in numerical simulation. The full wave finite element method is realized by commercial software COMSOL Multiphysics [23]. The effect of adding DLTG can be determined by comparing the absorption in silicon absorber layer to the reference structure without grating.

In the simulation, both illuminations with a transverse electric (TE) polarized plane wave (E-field pointed out of x–y plane (y-axis), along the grating direction) and the transverse magnetic (TM) polarized plane wave (H-field pointed along the grating direction) are considered. The current density is calculated according to the following equation:

$$J_{sc} = e \int_{400\,nm}^{1100\,nm} \frac{\lambda}{hc} EQE(\lambda) I_{AM1.5}(\lambda) d\lambda \tag{1}$$

where $EQE(\lambda) = p_{absorption}(\lambda)/p_{in}(\lambda)$ is external quantum efficiency, $I_{AM1.5}$ is the reference solar spectral irradiance (ASTM G-173). The absorption of Si absorber is calculated by $\omega \cdot \varepsilon''(\omega) \oint_v |E|^2 dv$, v is volume of silicon absorber layer, and $|E|^2$ is normalized light intensity at near field, ε'' is the imaginary part of dielectric function of crystal silicon, which is cited the experimental data of Paik [24].

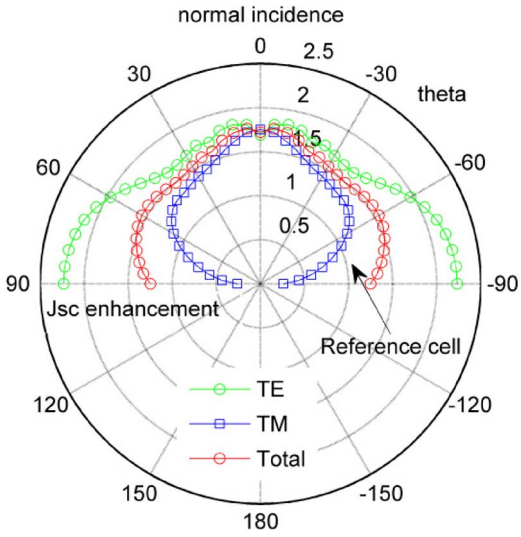

Fig. 2. Angular dependence of the short circuit current enhancement for designed structure of triangular grating.

The wavelength is considered from 400 nm to 1100 nm, which covers the full absorption band for crystal silicon solar cells.

3. Result and Discussion

The angular dependence of the short circuit current enhancement for the optimized grating is shown in Fig. 2. The optimal grating is consisted of silver triangular grating array with width of 40 nm, height of 130 nm, and period of 280 nm, coated with 45 nm Si_3N_4 layer. Photogenerated current in DLTG solar cells at each angle of incidence is divided by the current of reference cell at the same angle of incidence as DLTG solar cells.

Seen from Fig. 2, the solar cell covered by DLTG shows little sensibility to the angle of incidence, and retain an average of above 50% enhancement over 0 to 60 degrees. For incident illumination of TE polarization, the J_{sc} enhancement is above 100%, at the angle of incidence that are greater than 60 degrees. In the case of TM polarization, the maximum is about 75% at normal incidence. And the total enhancement reaches 76.8% at 5 degrees. Even at 60 degrees of incidence, the enhancement factor is as high as 50%. Such a performance of DLTG is as good as the rectangular grating coated with antireflection layer [22], which shows that optimized DLTG is an alternative structure for light trapping in plasmon-based solar cells. When the incident angle becomes bigger than 60 degrees, the current enhancement for TM illumination decreases rapidly due to both the LSPs and SPPs are sensitive to incident angle. On the contrary, when the incident angle becomes bigger than 60 degrees, the current enhancement for TE illumination become greater due to "moth eye" effect of Si_3N_4 grating array, which is with a relative high aspect ratio, 130/40, and thus less sensitive to the angle of incidence. It is worth noting that the insensitive of angle of incidence for DLTG solar cells is mainly due to the large current enhancement under TE illumination, resulting from the influence of antireflection coating.

To explore the mechanism of great improvement of absorption, the dispersion relationship of the planar waveguide structure without grating are investigated. Fig. 3 is the contour map of absorption enhancement versus the reciprocal vector of grating array, $k = 2\pi/p$. The corresponding wavelength and period are also labeled. In the mode analysis, the eigenvalues, Λ, are obtained firstly for each frequency, then the effective index, $n_{eff} = -I * \Lambda/k0$, and propagation constant, $\beta = imag(-\Lambda)$, are calculated. For the dispersion relationship (dots and dash line in Fig. 3), the wave vector of x-axis represents propagation constant, and the energy of y-axis indicates eigenfrequency.

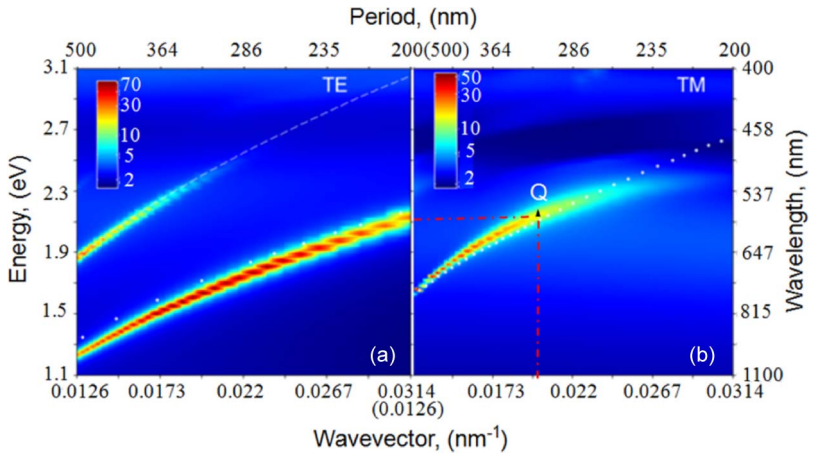

Fig. 3. Contour plot of absorption enhancement of solar cells versus the incident photon energy and reciprocal lattice vector of triangular grating array for TE illumination (a) and TM illumination (b). The dots and dashed lines represent dispersion characteristics of solar cells without grating. Dots correspond to the fundamental modes, and dashed lines represent repetitions of the fundamental mode with larger periods. The grating structure is 40 nm (width) by 130 nm (height), with period varying from 200 nm to 500 nm. Both modes in (a) and (b) are mainly waveguide modes, which are pith-dependent. Position Q is the absorption peak at 560 nm which is corresponding to the width 40 nm and period 310 nm.

As shown in Fig. 3, The absorption enhancement factor is strongly frequency-dependent and varies from 0.48 to 1 (the dark blue color) and 1 to the highest factor (the blue to red color). The color map is in logarithmic scale to show the lower values more clearly. As shown in Fig. 3(a), the maximum enhancement factor of absorption for TE illumination is 76 at 750 nm, which means 76 times the absorption of the reference cells without grating. Similarly, for TM illumination [Fig. 3(b)], there is also a ribbon-like band of maximal absorption, and the maximum value is 66, when the period is 491 nm and wavelength is 740 nm. It is important to note that the absorption band, shown in Fig. 3(b) for TM polarization, is pitch-dependent, which is attributed to the coupling of SPPs [25]. On the whole, the dispersion curves of waveguide coincide well with the band of maximal absorption in Si slab. This result shows the absorption enhancement for our grating is mainly attributed to improved coupling to guided modes.

In order to determine whether the localized mode affect the absorption enhancement or not, width-dependent absorption is examined. It is found that guide mode and localized mode both exist for TM illumination and only guide mode exist for TE illumination. As shown in Fig. 4(a), the red dots are in a straight line at 510 nm precisely, and the corresponding wavelength keeping still with the increasing of width, which is the distinct characteristic of guide mode undergoing Bloch-wave-like resonances [25]. Meanwhile, the circles in Fig. 4(a) form roughly a line around the resonance wavelength of 730 nm, which are Bloch-wave-like resonances too. These waveguide modes also appears for TM illumination, but the resonance wavelength shift slightly from 510 nm to 525 nm, which is due to the SPPs resonance. As shown in Fig. 4(b), the localized mode (circles) is strongly width-dependent, and the resonance wavelength red shift with increasing the width. The SPPs resonance of larger width is stronger in intensity than that of smaller width. On the contrary, the LSPs resonance of smaller width is much stronger in intensity than that of bigger width.

As the solid triangle shown in Fig. 4(b), when the width is fixed at 40 nm and period is 310 nm, the resonance wavelength occurs at about 560 nm. According to this, the equivalent position Q can also be located in Fig. 3(b), which falls into the maximal absorption band and above the dots line. It shows that the maximal absorption band is the contribution of both guide modes (dots line) and the localized modes (point-Q-like), and that the main contributor is determined by the profile parameters such as the width and period. From the comparison of point Q, dots line and the absorption band in Fig. 3(b), it can also be concluded that the discrepancy of absorption band and analytical solution of guide modes (dots line) is due to localized modes which can excited by metallic grating easily under

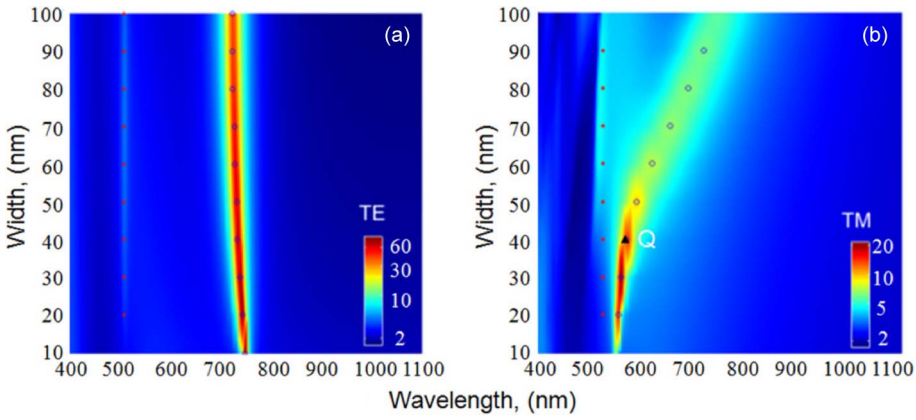

Fig. 4. Contour plots of absorption enhancement versus the width and incident wavelength for TE illumination (a) and TM illumination (b). The red dots and blue circles are peaks of absorption, which indicate the waveguide modes and localized modes. The simulation structure is with period of 310 nm, height of 130 nm, and width varied from 10 to 100 nm. While both the dots and circles in (a) are waveguide modes (affected little by changing of width), the dots and circles in (b) represent waveguide modes and localized modes (width-dependent), respectively. Position Q is the absorption peak at 560 nm which is corresponding to the width 40 nm and period 310 nm.

TM illumination. That is, the absorption enhancement is mainly stemmed from guide modes on the whole as discussion above, and also stemmed from localized modes at some certain condition.

The excellent performance of DLTG benefits not only from the surface plasmon resonance, but also from the antireflecting property of dielectric coating. The contribution of antireflection is mainly reflected in absorption enhancement for TE illumination, as shown in Figs. 3(a) and 4(a), and the contribution of surface plasmon resonance is reflected in absorption gaining for TM illumination, shown in Figs. 3(b) and 4(b).

To demonstrate the influence of DLTG on light trapping in thin film solar cells, back reflector is not considered in this paper. In addition, to extract the current carriers excited by absorbed photons, front and back electrodes are also needed. Therefore, one possible prototype of DLTG solar cells is, from top to bottom, DLTG(Si_3N_4/Ag)/Si/Al, where the silver layer in DLTG should be exposed at some places functioning as front contact as well, and Al films behind take the dual role of both back reflector and back electrode at the same time. It is clear that more exposure of silver layer will improve the carrier collection at front contact, however, too much exposure of silver grating will impair the antireflection effect of dielectric coating. Thus, there is a tradeoff between light trapping and carrier collection in such DLTG solar cells. Furthermore, the proposed model belongs to plasmon-based solar cells, the plasmon structures of which are excellent in concentrating and propagating light in subwavelength size, and thus it is more favorable for thin film solar cells, and the advantage of plasmon solar cells will be diminished as the absorber is becoming thicker. Even so, DLTG structures are still an excellent alternative scheme for light trapping in plasmon-based solar cells, and are a good platform to engineer the light absorption and propagation in optoelectronic devices.

4. Conclusion

In conclusion, a type of plasmonic solar cells with DLTG is proposed and investigated. Covered by such a DLTG structure, the enhancement of short circuit current density can reach 76.8% at 5 degrees, obtained from the average on both TM and TE polarizations under AM 1.5 global illuminations. With increasing the angle of solar illumination, the enhancement factor of current reduces slightly. But even at as large as 60 degrees, the enhancement factor is as high as proximately 50%. The mode analysis confirms that the great optical absorption enhancement is attributed to improved coupling to both guided modes and localized mode. The DLTG structure benefits both the advantages of surface plasmon coupling and subwavelength antireflecting. This is an important way toward the high-efficiency plasmonic photovoltaics.

References

[1] H. A. Atwater and A. Polman, "Plasmonics for improved photovoltaic devices," *Nat. Mater.*, vol. 9, no. 3, pp. 205–213, Mar. 2010.
[2] F. J. Beck, A. Polman, and K. R. Catchpole, "Tunable light trapping for solar cells using localized surface plasmons," *J. Appl. Phys.*, vol. 105, no. 11, p. 114 310, 2009.
[3] K. R. Catchpole and A. Polman, "Design principles for particle plasmon enhanced solar cells," *Appl. Phys. Lett.*, vol. 93, no. 19, p. 191 113, Nov. 2008.
[4] W. E. I. Sha, W. C. H. Choy, and W. C. Chew, "Angular response of thin-film organic solar cells with periodic metal back nanostrips," *Opt. Lett.*, vol. 36, no. 4, pp. 478–480, Feb. 2011.
[5] Y. Yeh, Y. Wang, and J. Li, "Enhancement of the optical transmission by mixing the metallic and dielectric nanoparticles atop the silicon substrate," *Opt. Exp.*, vol. 19, no. Supplement 2, pp. A80–A94, Mar. 2011.
[6] J. Zhu, M. Xue, H. Shen, Z. Wu, S. Kim, J. Ho, A. Hassani-Afshar, B. Zeng, and K. L. Wang, "Plasmonic effects for light concentration in organic photovoltaic thin films induced by hexagonal periodic metallic nanospheres," *Appl. Phys. Lett.*, vol. 98, no. 15, pp. 151 110–151 110-3, Apr. 2011.
[7] C. Hägglund, M. Zäch, and B. Kasemo, "Enhanced charge carrier generation in dye sensitized solar cells by nanoparticle plasmons," *Appl. Phys. Lett.*, vol. 92, no. 1, p. 013 113, Jan. 2008.
[8] I. Diukman, L. Tzabari, N. Berkovitch, N. Tessler, and M. Orenstein, "Controlling absorption enhancement in organic photovoltaic cells by patterning Au nano disks within the active layer," *Opt. Exp.*, vol. 19, no. S1, pp. A64–A71, Jan. 2011.
[9] S. Tsai, M. Ballarotto, D. B. Romero, W. N. Herman, H. Kan, and R. J. Phaneuf, "Effect of gold nanopillar arrays on the absorption spectrum of a bulk heterojunction organic solar cell," *Opt. Exp.*, vol. 18, no. Supplement 4, pp. A528–A535, Nov. 2010.
[10] Y. A. Akimov and W. S. Koh, "Design of plasmonic nanoparticles for efficient subwavelength light trapping in thin-film solar cells," *Plasmonics*, vol. 6, no. 1, pp. 155–161, Mar. 2011.
[11] M. Kang, T. Xu, H. J. Park, X. Luo, and L. J. Guo, "Efficiency enhancement of organic solar cells using transparent plasmonic Ag nanowire electrodes," *Adv. Mater.*, vol. 22, no. 39, pp. 4378–4383, Oct. 2010.
[12] O. El Daif, E. Drouard, G. Gomard, A. Kaminski, A. Fave, M. Lemiti, S. Ahn, S. Kim, P. Roca i Cabarrocas, H. Jeon, and C. Seassal, "Absorbing one-dimensional planar photonic crystal for amorphous silicon solar cell," *Opt. Exp.*, vol. 18, no. S3, pp. A293–A299, Sep. 2010.
[13] R. A. Pala, J. White, E. Barnard, J. Liu, and M. L. Brongersma, "Design of plasmonic thin-film solar cells with broadband absorption enhancements," *Adv. Mater.*, vol. 21, no. 34, pp. 3504–3509, Sep. 2009.
[14] M. A. Sefunc, A. K. Okyay, and H. V. Demir, "Volumetric plasmonic resonator architecture for thin-film solar cells," *Appl. Phys. Lett.*, vol. 98, no. 9, p. 093 117, Mar. 2011.
[15] W. Wang, S. Wu, K. Reinhardt, Y. Lu, and S. Chen, "Broadband light absorption enhancement in thin-film silicon solar cells," *Nano Lett.*, vol. 10, no. 6, pp. 2012–2018, Jun. 2010.
[16] Z. Fan, H. Razavi, J. Do, A. Moriwaki, O. Ergen, Y. Chueh, P. Leu, J. Ho, T. Takahashi, L. Reichertz, S. Neale, K. Yu, M. Wu, J. Ager, and A. Javey, "Three-dimensional nanopillar-array photovoltaics on low-cost and flexible substrates," *Nat. Mater.*, vol. 8, no. 8, pp. 648–653, Aug. 2009.
[17] H. Zhao, J. Zhang, G. Liu, and N. Tansu, "Surface plasmon dispersion engineering via double-metallic Au/Ag layers for III-nitride based light-emitting diodes," *Appl. Phys. Lett.*, vol. 98, no. 15, p. 151 115, Apr. 2011.
[18] J. Henson, A. Bhattacharyya, T. D. Moustakas, and R. Paiella, "Controlling the recombination rate of semiconductor active layers via coupling to dispersion-engineered surface plasmons," *J. Opt. Soc. Amer. B, Opt. Phys.*, vol. 25, no. 8, pp. 1328–1335, Aug. 2008.
[19] J. Jewell, D. Simeonov, S.-C. Huang, Y.-L. Hu, S. Nakamura, J. Speck, and C. Weisbuch, "Double embedded photonic crystals for extraction of guided light in light-emitting diodes," *Appl. Phys. Lett.*, vol. 100, no. 17, pp. 171105-1–171105-4, Apr. 2012.
[20] X.-H. Li, R. Song, Y.-K. Ee, P. Kumnorkaew, J. F. Gilchrist, and N. Tansu, "Light extraction efficiency and radiation patterns of III-Nitride light-emitting diodes with colloidal microlens arrays with various aspect ratios," *IEEE Photon. J.*, vol. 3, no. 3, pp. 489–499, Jun. 2011.
[21] N. Fahim, Z. Ouyang, Y. Zhang, B. Jia, Z. Shi, and M. Gu, "Efficiency enhancement of screen-printed multicrystalline silicon solar cells by integrating gold nanoparticles via a dip coating process," *Opt. Mater. Exp.*, vol. 2, no. 2, pp. 190–204, Feb. 2012.
[22] J. N. Munday and H. A. Atwater, "Large integrated absorption enhancement in plasmonic solar cells by combining metallic gratings and antireflection coatings," *Nano Lett.*, vol. 11, no. 6, pp. 2195–2201, Jun. 2011.
[23] C.-H. Lu, C.-C. Lan, Y.-L. Lai, Y.-L. Li, and C.-P. Liu, "Enhancement of green emission from InGaN/GaN multiple quantum wells via coupling to surface plasmons in a two-dimensional silver array," *Adv. Funct. Mater.*, vol. 21, no. 24, pp. 4719–4723, Dec. 2011.
[24] E. D. Palik, *Handbook of Optical Constants of Solids*. Boston, MA: Academic, 1985.
[25] Z. Sun and X. Zuo, "Resonances on a metal surface with interspaced ultra-thin metal gratings," *Plasmonics*, vol. 6, pp. 83–89, 2010.